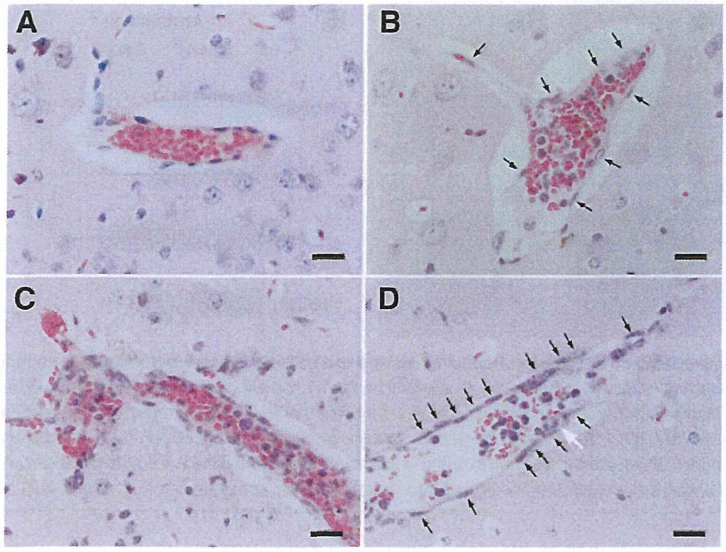

Figure 3 Brain histopathology. (A) CGN group. No apparent lesions are observed (Haematoxylin-Eosin stain). Bar, 20 μm. **(B)** PbN group. Microthrombus consisting of fibrin pigmented RBCs and accumulated mononuclear cells, is observed. Perivascular infiltration of inflammatory cells is not observed. Vascular endothelium is not hyperplastic (arrows indicate endothelial cells). Bar, 20 μm. **(C)** PbCGN group. Microthrombus consisting of fibrin, pigmented RBCs, pigmented macrophages, and mononuclear cells is observed. Perivascular infiltration of inflammatory cells, haemorrhage in perivascular space, and hyperplastic vascular endothelium are also observed. Bar, 20 μm. **(D)** PbCGN group. Infected RBCs and inflammatory cells can be seen within the blood vessels of the cerebrum. Note the hyperplastic endothelium, characterized by increased number of endothelial cells (arrow). Adhesive Pb-laden macrophages (shown by white arrow) can also be seen. Bar, 20 μm.

in the number of intracerebral haemorrhages between the PbN and PbCGN groups. However, haemorrhages were observed in all regions of the brains of all of the PbCGN mice, whereas they were observed in only half of the PbN mice tested (Table 1). These findings are consistent with the increased severity of the pathology in the PbCGN mice relative to the PbN mice.

Assessment of vascular leakage at the blood–brain barrier by using Evans blue dye perfusion

To further evaluate the effects of λ-carrageenan on the integrity of blood–brain barrier (BBB), and its contribution to the early death of the mice infected with *P. berghei* ANKA, the permeability of the blood–brain barrier was assessed by using Evans blue assay. Representative images of the brains of mice from each group are shown in Figure 4. The brains of the PbN and PbCGN mice (Figure 4C and D, respectively) absorbed the dye, indicating increased permeability of the blood–brain barrier compared with that of the brains of normal mice and CGN mice (Figure 4A and B, respectively). As expected, CGN mice showed increased levels of blood–brain barrier leakage relative to the levels in the brains of normal mice. However, there were no statistically significant differences in the levels of Evans blue dye leakage from the mouse brains between the PbN and PbCGN groups (Figure 4E). These results indicate that not only the altered integrity of blood–brain barrier but also other factors may lead to this severe complication of malaria in mice infected with *P. berghei* ANKA.

Table 1 Intracerebral haemorrhage counts

Haemorrhage score	PbN				PbCGN				Mann–Whitney *P*
	A	B	C	D	E	F	G	H	
Frontal Lobe	2	0	0	4	6	4	9	3	0.05755
Diencephalon	5	0	0	1	6	4	9	3	0.1059
Occipital Lobe	4	2	0	6	2	4	7	2	0.6552
Cerebellum	5	0	0	1	4	6	4	4	0.1367
Total	16	2	0	12	14	19	27	11	0.1489

Statistically significant differences in intracerebral haemorrhage counts were determined by using the Mann–Whitney test. Values were considered to be significantly different when the *P* value was less than 0.05.

Discussion

Here, the *in vivo* efficacy and safety of λ-carrageenan as an anti-malarial drug was evaluated. The results show that λ-carrageenan poorly inhibited the growth of *P. berghei* ANKA in BALB/c mice and caused more severe brain lesions, leading to the early death of the mice. BALB/c mice, which are considered to be relatively resistant to the consequences of cerebral malaria caused by the ANKA strain of *P. berghei* [10,17-19], were chosen as model to assess the effects of the administration of λ-carrageenan to the development of clinical signs associated with cerebral malaria. Both groups were shown to develop a high parasitaemia, but the

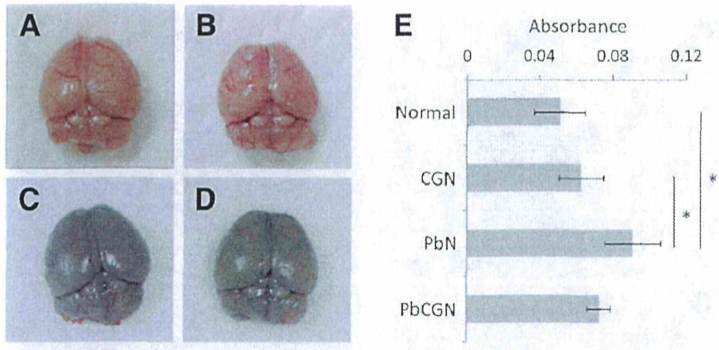

Figure 4 Assessment of vascular leakage at the blood–brain barrier by use of Evans blue dye perfusion. Two hundred microliters of 1% Evans blue dye was injected into the tail veins of each mice on day 5 post-infection. After 1 h, the mice were sacrificed using terminal isoflurane anesthesia and the brains were collected. Representative brains are shown: **(A)** Normal healthy mouse (N), **(B)** Carrageenan-treated mouse (CGN), **(C)** *P. berghei* ANKA-infected, untreated mouse (PbN), **(D)** *P. berghei* ANKA-infected, carrageenan-treated mouse (PbCGN). **(E)** The mean absorbances at 600 nm wavelength and standard deviations of extracted dye after placing the brains in 4% paraformaldehyde for 48 h are shown for each group. Statistically significant differences in mean absorbances were determined by using Tukey's multiple comparison test (*: *P* value < 0.05, ns: not significant).

infected BALB/c mice treated with λ –carrageenan showed more signs related to ECM and died earlier than the untreated mice. The attempts to show that λ-carrageenan treatment could cause more severe cerebral malaria through histopathology and Evans blue dye assays revealed almost the same results for both groups of infected mice. The levels of blood–brain barrier leakage were similar between the *P. berghei*-infected mice that were mock-treated and those that were administered λ-carrageenan; and the histopathological findings on the brains show the presence of intracranial haemorrhages for both groups. It is important to note that with the small sample size used in this study, the statistical data presented here should be interpreted with caution [20-22].

It is also possible that although the clinical signs associated with ECM in the untreated group were not observed, these mice may also have developed ECM, as reported by Neill and Hunt [23]. It will be interesting to explore the underlying mechanisms as to why clear neurological signs were not as evident in the untreated group given that there was hyperparasitaemia, leakage in the BBB and presence of intracranial haemorrhages. These results indicate that there may be other factors involved in the early death of mice treated with λ-carrageenan during *P. berghei* ANKA infection. One can also consider the possibility that the hyperplastic endothelium of the brain blood vessels compensated for the blood–brain barrier leakage in the PbCGN group.

Lambda-carrageenan is known to induce inflammatory pain and to alter the permeability of the blood–brain barrier in several animal models [9,24]. Moreover, administration of λ-carrageenan increases the expression of ICAM-1, which plays a key role in the sequestration of iRBCs in cerebral malaria under experimental and natural conditions [25,26].

By contrast, λ-carrageenan is known to activate the innate immunity that depends on Toll-like receptor 4 (TLR4) and Myd88 [5]. Given that the activation of TLR4/Myd88 signaling causes acute inflammatory injury [27], one could argue that the early deaths of mice treated with λ-carrageenan during the *P. berghei* ANKA infection could be attributed to the dysregulation of innate immunity rather than the dysfunction of the blood–brain barrier. Further studies are warranted to elucidate the molecular basis of this exacerbation of pathology.

Malaria remains a threat to human health and there is an urgent need to develop and test novel compounds. The results presented here suggest that λ-carrageenan, a sulphated polysaccharide which is a common food additive and ingredient in household products and has been found to inhibit the invasion of red blood cells by malaria merozoites *in vitro*, may be unsuitable for the treatment of clinical malaria.

However, other sulphated polysaccharides, including heparin, fucoidan, and dextran sulfate [28,29] have shown promising *in vitro* anti-malarial activity. An example is the previous report on gellan sulfate [30] that demonstrated that chemical modification, namely, sulphation, could change the characteristics of these compounds. Given that these polysaccharides are still considered promising potential anti-malaria drugs, chemical modification might decrease the side effects of such compounds.

Conclusion

This study shows the potential toxicity of λ-carrageenan as an antimalarial using the BALB/c mice as model of

ECM. We find the usefulness of this rodent model in elucidating CM pathogenesis and evaluating promising antimalarial candidates *in vivo* and more importantly the safety profile of anti-malarial compounds that could not be envisaged if only *in vitro* experiments were conducted.

Abbreviations

CM: Cerebral malaria; ECM: Experimental cerebral malaria; HCM: Human cerebral malaria; BBB: Blood–brain barrier; iRBCs: Infected red blood cells; H-E: Haematoxylin-eosin stain.

Competing interests

The authors declare that they have no competing interests.

Authors' contributions

FCR and KK designed the study. FCR performed all of the animal experiments and wrote the manuscript. RT conducted the statistical studies and co-wrote the manuscript. SC, NH, and YK prepared the histopathology slides and performed all of the histopathological examinations. TS, HT, FM, A. Ishiwa, A. Inomata, and TH contributed to the data analysis. KK edited the manuscript and supervised the study. All authors have read and approved the final version of the manuscript.

Acknowledgements

This study was supported by Grants-in-Aids for Young Scientists, and Scientific Research on Innovative Areas (3308) from the Ministry of Education, Culture, Science, Sports, and Technology (MEXT) and for Research on global health issues from the Ministry of Health, Labour, and Welfare of Japan, by Bio-oriented Technology Research Advancement Institution (BRAIN), by the Naito Foundation, and by the Programme to Disseminate Tenure Tracking System from the Japan Science and Technology Agency (JST).
We would also like to thank Dr. Maria Shirley Herbas of the NRCPD, Obihiro University of Agriculture and Veterinary Medicine for providing training on tissue handling and collection.

Author details

[1]Department of Veterinary Microbiology, Graduate School of Agricultural and Life Sciences, The University of Tokyo, 1-1-1 Yayoi, Bunkyo-ku, Tokyo 113-8657, Japan. [2]National Research Center for Protozoan Diseases, Obihiro University of Agriculture and Veterinary Medicine, Obihiro 080-8555, Hokkaido, Japan. [3]Department of Basic Veterinary Medicine, Obihiro University of Agriculture and Veterinary Medicine, Obihiro 080-8555, Hokkaido, Japan. [4]Department of Veterinary Paraclinical Sciences, College of Veterinary Medicine, University of the Philippines Los Baños, Laguna 4031, Philippines.

Received: 1 September 2014 Accepted: 7 December 2014
Published: 11 December 2014

References

1. Adams Y, Smith SL, Schwartz-Albiez R, Andrews KT: **Carrageenans inhibit the *in vitro* growth of *Plasmodium falciparum* and cytoadhesion to CD36.** *Parasitol Res* 2005, **97**:290–294.
2. James MA, Alger NE: ***Plasmodium berghei*: effect of carrageenan on the course of infection in the A/J mouse.** *Int J Parasitol* 1981, **11**:217–220.
3. Moyana TN, Lalonde JM: **Carrageenan-induced intestinal injury in the rat –a model for inflammatory bowel disease.** *Ann Clin Lab Sci* 1990, **20**:420–426.
4. Merlo S, Dolovich J, Listgarten C: **Anaphylaxis to carrageenan: a pseudo-latex allergy.** *J Allergy Clin Immunol* 1995, **95**:933–936.
5. Tsuji RF, Hoshino K, Noro Y, Tsuji NM, Kurokawa T, Masuda T, Akira S, Nowak B: **Suppression of allergic reaction by λ-carrageenan: toll-like receptor 4/MyD88-dependent and -independent modulation of immunity.** *Clin Exp Allergy* 2003, **33**:249–258.
6. Tobacman JK, Wallace RB, Zimmerman MB: **Consumption of carrageenan and other water-soluble polymers used as food additives and incidence of mammary carcinoma.** *Med Hypotheses* 2001, **56**:589–598.
7. Silva FRF, Dore CMPG, Marques CT, Nascimento MS, Benevides NMB, Rocha HAO, Chavante SF, Leite EL: **Anticoagulant activity, paw edema and pleurisy induced carrageenan: action of major types of commercial carrageenans.** *Carbohydr Polym* 2010, **79**:26–33.
8. Suralkar AA, Sarda PS, Ghaisas MM, Thakare VN, Deshpande AD: **In-vivo animal models for evaluation of anti-inflammatory activity.** *Pharmainfonet* 2008, **6**: http://www.pharmainfo.net/reviews/vivo-animal-models-evaluation-anti-inflammatory-activity. Accessed July 8, 2014.
9. Huber JD, Hau VS, Borg L, Campos CR, Egleton RD, Davi TP: **Blood–brain barrier tight junctions are altered during a 72-h exposure to λ-carrageenan-induced inflammatory pain.** *Am J Physiol Heart Circ Physiol* 2002, **283**:H1531–H1537.
10. Rénia L, Howland SW, Claser C, Charlotte Gruner A, Suwanarusk R, Hui Teo T, Russel B, Ng LF: **Cerebral malaria: mysteries at the blood–brain barrier.** *Virulence* 2012, **3**:193–201.
11. Aikawa M, Iseki M, Barnwell JW, Taylor D, Oo MM, Howard RJ: **The pathology of cerebral malaria.** *Am J Trop Med Hyg* 1990, **43**:30–37.
12. van der Heyde HC, Nolan J, Combes V, Gramaglia I, Grau GE: **A unified hypothesis for the genesis of cerebral malaria: sequestration, inflammation and hemostasis leading to microcirculatory dysfunction.** *Trends Parasitol* 2006, **22**:503–508.
13. Ponsford MJ, Medana IM, Prapansilp P, Hien TT, Lee SJ, Dondorp AM, Esiri MM, Day NP, White NJ, Turner GD: **Sequestration and microvascular congestion are associated with coma in human cerebral malaria.** *J Infect Dis* 2012, **205**:663–671.
14. Jennings VM, Actor JK, Lal AA, Hunter RL: **Cytokine profile suggesting that murine cerebral malaria is an encephalitis.** *Infect Immun* 1997, **65**:4883–4887.
15. Bopp SER, Rodrigo E, Gonzalez-Paez GE, Frazer M, Barnes SW, Valim C, Watson J, Walker JR, Schemdt C, Winzeler EA: **Identification of the *Plasmodium berghei* resistance locus 9 linked to survival on chromosome 9.** *Malar J* 2013, **12**:316.
16. Carroll RW, Wainwright MS, Kim KY, Kidambi T, Gomez ND, Taylor T, Haldar K: **A rapid murine coma and behavior scale for quantitative assessment of murine cerebral malaria.** *PLoS One* 2010, **5**:e13124.
17. Nacer A, Movila A, Baer K, Mikolajczak SA, Kappe SHI, Frevert U: **Neuroimmunological blood brain barrier opening in experimental cerebral malaria.** *PLoS Pathog* 2012, **8**:e1002982. doi:10.1371/journal.ppat.1002982.
18. Schmidt KE, Schumak B, Specht S, Dubben B, Limmer A, Hoerauf A: **Induction of pro-inflammatory mediators in *Plasmodium berghei* infected BALB/c mice breaks blood–brain-barrier and leads to cerebral malaria in an IL-12 dependent manner.** *Microb Infect* 2011, **13**:828–836.
19. Taylor-Robinson AW: **Validity of modelling cerebral malaria in mice: argument and counter argument.** *J Neuroparasitol* 2010, **1**:N100601. doi:10.4303/jnp/N100601. Accessed July 8, 2014.
20. Bacchetti P, Deeks SG, McCune JM: **Breaking free of sample size dogma to perform innovative translational research.** *Sci Transl Med* 2011, **3**:87ps24.
21. Liu PT: **Extremely small sample size in some toxicity studies: an example from the rabbit eye irritation test.** *Regul Toxicol Pharmacol* 2001, **33**:187–191.
22. De Winter JCF: **Using the student's t-test with extremely small sample sizes.** *PARE* 2013, **18**:1–12.
23. Neill AL, Hunt NH: **Pathology of fatal and resolving *Plasmodium berghei* cerebral malaria in mice.** *Parasitology* 1992, **105**:165–175.
24. Huber JD, Campos CR, Mark KS, Davis TP: **Alterations in blood–brain barrier ICAM-1 expression and brain microglial activation after lambda-carrageenan-induced inflammatory pain.** *Am J Physiol Heart Circ Physiol* 2006, **290**:H732–H740.
25. Shear HL, Shear HL, Marino MW, Wanidworanun C, Berman JW, Nagel RL: **Correlation of increased expression of intercellular adhesion molecule-1, but not high levels of tumor necrosis factor-alpha, with lethality of *Plasmodium yoelii* 17XL, a rodent model of cerebral malaria.** *Am J Trop Med Hyg* 1998, **1998**(59):852–858.
26. Cserti-Gazdewich CM: ***Plasmodium falciparum* malaria and carbohydrate blood group evolution.** *ISBT Sci Ser* 2010, **5**:256–266. doi:10.1111/j.1751-2824.2010.01380.x.
27. Zhu HT, Bian C, Yuan JC, Chu WH, Xiang X, Chen F, Wang CS, Feng H, Lin JK: **Curcumin attenuates acute inflammatory injury by inhibiting the TLR4/MyD88/NF-κB signaling pathway in experimental traumatic brain injury.** *J Neuroinflammation* 2014, **11**:59. doi: 10.1186/1742-2094-11-59.
28. Clark DL, Su S, Davidson EA: **Saccharide anions as inhibitors of the malaria parasite.** *Glycoconj J* 1997, **14**:473–479.

29. Xiao L, Yang C, Patterson PS, Udhayakumar V, Lal AA: **Sulfated polyanions inhibit invasion of erythrocytes by *Plasmodium* merozoites and cytoadherence of endothelial cells to parasitized erythrocytes.** *Infect Immun* 1996, **64**:1373–1378.
30. Recuenco FC, Kobayashi K, Ishiwa A, Enomoto-Rogers Y, Fundador NGV, Sugi T, Takemae H, Iwanaga T, Murakoshi F, Gong H, Inomata A, Horimoto T, Iwata T, Kato K: **Gellan sulfate inhibits *Plasmodium falciparum* growth and invasion of red blood cells *in vitro*.** *Sci Rep* 2014, **4**:4723. doi:10.1038/srep04723.

doi:10.1186/1475-2875-13-487
Cite this article as: Recuenco *et al.*: Lambda-carrageenan treatment exacerbates the severity of cerebral malaria caused by *Plasmodium berghei* ANKA in BALB/c mice. *Malaria Journal* 2014 13:487.

Analytical Biochemistry 464 (2014) 9–11

Contents lists available at ScienceDirect

Analytical Biochemistry

journal homepage: www.elsevier.com/locate/yabio

Notes & Tips

Microplate assay for screening *Toxoplasma gondii* bradyzoite differentiation with DUAL luciferase assay

Tatsuki Sugi [a], Tatsunori Masatani [a,b], Fumi Murakoshi [a,c], Shin-ichiro Kawazu [a], Kentaro Kato [a,c,*]

[a] National Research Center for Protozoan Diseases, Obihiro University of Agriculture and Veterinary Medicine, Obihiro, Hokkaido 080-8555, Japan
[b] Transboundary Animal Diseases Center, Joint Faculty of Veterinary Medicine, Kagoshima University, Kagoshima 890-0065, Japan
[c] Department of Veterinary Microbiology, Graduate School of Agricultural and Life Sciences, University of Tokyo, Bunkyo-ku, Tokyo 113-8657, Japan

ARTICLE INFO

Article history:
Received 15 May 2014
Received in revised form 18 June 2014
Accepted 19 June 2014
Available online 30 June 2014

Keywords:
Bradyzoite
DUAL luciferase assay
High-throughput screening
Reporter parasite
Toxoplasma gondii

ABSTRACT

Toxoplasma gondii can differentiate into tachyzoites or bradyzoites. To accelerate the investigation of bradyzoite differentiation mechanisms, we constructed a reporter parasite, PLK/DLUC_1C9, for a high-throughput assay. PLK/DLUC_1C9 expressed firefly luciferase under the bradyzoite-specific BAG1 promoter. Firefly luciferase activity was detected with a minimum of 10^2 parasites induced by pH 8.1. To normalize bradyzoite differentiation, PLK/DLUC_1C9 expressed Renilla luciferase under the parasite's α-tubulin promoter. Renilla luciferase activity was detected with at least 10^2 parasites. By using PLK/DLUC_1C9 with this 96-well format screening system, we found that the protein kinase inhibitor analogs, bumped kinase inhibitors 1NM-PP1, 3MB-PP1, and 3BrB-PP1, had bradyzoite-inducing effects.

The infection prevalence of *Toxoplasma gondii*, a protozoan parasite in Apicomplexa, is high all over the world [1]. When *T. gondii* infects humans, it causes toxoplasmosis in infants [2] and immunocompromised patients [3]. *T. gondii* can differentiate into two types of cells in its intermediate host animals: a fast-replicating tachyzoite and a slow-replicating dormant bradyzoite in the cyst. Cell differentiation from tachyzoite to bradyzoite is related to infectious cyst formation in meat production animals (tachyzoite to bradyzoite) and to recurrence of latent infection in acquired immunodeficient patients (bradyzoite to tachyzoite) [4]. Bradyzoite-specific gene expression has been well documented via transcriptome analysis using *in vitro* systems [5] and *in vivo* cysts [6]. However, how the stress response is transduced and which signals lead to the transcriptional changes are not yet fully understood. To answer these questions, a high-throughput screening system to identify factors that affect bradyzoite differentiation would be a powerful tool.

A major requirement for bradyzoite differentiation screening is the availability of a robust, easy, and sensitive detection method. Moreover, normalization of bradyzoite-specific value with the parasite number is needed because bradyzoite-inducing conditions tend to influence the parasite growth itself [7]. A widely used assay for bradyzoite differentiation uses real-time quantitative reverse transcription polymerase chain reaction analysis of bradyzoite-specific gene expression with normalization by constitutively expressed tubulin messenger RNA levels [8]. Several groups have reported the transgenic parasite for investigating bradyzoite differentiation based on fluorescent reporter systems [9,10] and a luciferase assay system [5,11]. Several groups have reported transgenic parasites for investigating bradyzoite differentiation based on fluorescent reporter systems [9,10] and a luciferase assay system [5,11]. However, the fluorescent reporter systems lack sensitivity, and the luciferase assay lacks a normalization method unless transient transfection is employed before every assay.

In the current report, we describe a new reporter system, named pDUALUCI, that expresses firefly luciferase under the control of the bradyzoite-specific BAG1 [TGME49_259020] promoter as well as Renilla luciferase under the control of the constitutively expressed α-tubulin TUBA1 [TGME49_316400] promoter (Fig. 1A). Detailed plasmid construction information is provided in the online supplementary material. Host Vero cells and parasites were maintained as described elsewhere [12]. Plasmid DNA (20 μg) was linearized with *Not*I and transfected into 1.0×10^6 cells of the PLK/hxgprt$^-$ strain (National Institutes of Health AIDS Reagent Program, No. 2860) [12]; stable transgenic parasites were selected by 50 μg/ml mycophenolic acid and 50 μg/ml xanthine and were then cloned by limiting dilution as described elsewhere [13]. A parasite

* Corresponding author at: National Research Center for Protozoan Diseases, Obihiro University of Agriculture and Veterinary Medicine, Obihiro, Hokkaido 080-8555, Japan. Fax: +81 155 49 5646.
E-mail address: kkato@obihiro.ac.jp (K. Kato).

http://dx.doi.org/10.1016/j.ab.2014.06.018
0003-2697/

A

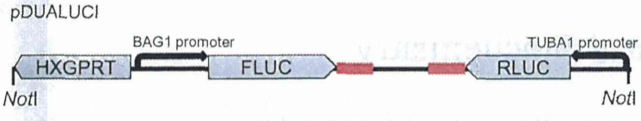

B

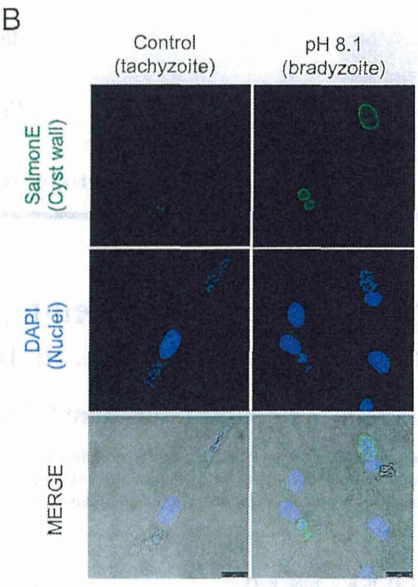

C

Detection range for the luciferase reporter activity

Condition	Cell number	Firefly Luciferase	Renilla luciferase
Tachyzoite	1.4E+05	2.7E+02 (±4.5E+00)	2.0E+06 (±3.3E+04)
	1.2E+04	N/D	2.1E+05 (±6.1E+03)
	1.1E+03	N/D	2.0E+04 (±7.3E+02)
	1.0E+02	N/D	1.8E+03 (±8.0E+01)
Bradyzoite	1.4E+05	8.1E+05 (±2.4E+04)	3.5E+06 (±4.4E+04)
	1.3E+04	8.2E+04 (±3.7E+03)	3.8E+05 (±1.3E+04)
	1.2E+03	7.8E+03 (±2.1E+02)	3.8E+04 (±1.9E+03)
	1.1E+02	7.3E+02 (±4.1E+01)	3.5E+03 (±1.5E+02)

Fig.1. Firefly luciferase expression by PLK/DLUC_1C9 is dependent on bradyzoite induction. (A) Schematic diagram of the DNA construct used to make PLK/DLUC_1C9. The *NotI sites used to linearize the plasmid are shown. Arrows show the directions of transcription. The diagram does not reflect the gene length. Red boxes show the terminator* sequence from 3′ UTR (untranslated region) of TgGRA2. (B) PLK/DLUC_1C9 can differentiate to bradyzoites. The cyst wall was stained with a SalmonE monoclonal antibody. Nuclei were stained with DAPI (4′,6-diamidino-2-phenylindole). The light fields combined with the fluorescent channels are shown as a merge. Scale bars = 25 μm. (C) Tachyzoites and bradyzoites were purified and counted by using a hemocytometer. The cell number denotes the parasite number in the lysate for the luciferase assay. Data are averages with standard deviations from three technical replicates. Values below the background average plus three times the background standard deviation are presented as N/D (not detected). (For interpretation of the reference to color in this figure legend, the reader is referred to the Web version of this article.)

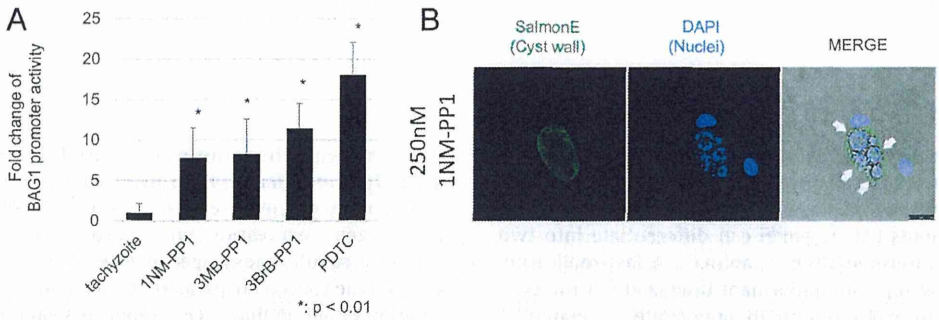

Fig.2. A 96-well microplate assay for bradyzoite differentiation. (A) 80 μM PDTC; 250 nM 1NM-PP1, 3MB-PP1, and 3BrB-PP1; and control medium containing dimethyl sulfoxide (final 0.1%, v/v) were used for the parasite treatment. BAG1 promoter activity was calculated by dividing the firefly luciferase activity by the Renilla luciferase activity. Fold changes in the bradyzoite promoter activity from the control sample are shown. Error bars show the standard deviations from independent quadruplicate experiments. An asterisk (*) indicates a *P* value < 0.01 by Student *t* test between the treatment and tachyzoite control. (B) 1NM-PP1 (250 nM) induces cyst wall formation and inhibits normal parasite growth. HFF cells infected by PLK/DLUC_1C9 were treated with 250 nM 1NM-PP1 from 2 h after parasite inoculation for 4 days. The cyst wall was stained with SalmonE monoclonal antibody. Nuclei were stained with DAPI (4′,6-diamidino-2-phenylindole). The light field and the fluorescent channels are shown as a merge. Scale bars = 25 μm. Arrows show the abnormally large cells in the parasitophorous vacuole.

clone, which exhibited the highest luciferase luminescence, was designated as PLK/DLUC_1C9. To determine whether PLK/DLUC_1C9 could differentiate to bradyzoites, we observed cyst wall formation. Human foreskin fibroblast (HFF)[1] cells were maintained as described elsewhere [12]. For bradyzoite induction, PLK/DLUC_1C9-infected HFF cells were treated with 1% fetal calf serum in Dulbecco's modified Eagle's medium with 25 mM Hepes (pH 8.1) without $NaHCO_3$ from 2 h after parasite inoculation and were incubated in humid air for 4 days. The cells were then fixed with 4% paraformaldehyde and stained with an anti-CST1 SalmonE monoclonal antibody as described elsewhere [14]. The pH 8.1 medium-treated PLK/DLUC_1C9 showed cyst wall staining, whereas the tachyzoite control showed no staining in the parasitophorous vacuole membranes (Fig. 1B). To measure the detection limit of the luciferase assay, we measured the luciferase activity of purified parasites. Parasite pellets were lysed in Passive Lysis Buffer (Promega) and used in the luciferase assay according to the instructions provided by the manufacturer of the Dual-Luciferase Reporter Assay System (Promega) using LUMAT LB9507 (Berthold). The background luminescence value from the lysis buffer containing no parasites was subtracted from the raw values and estimated to give relative luminescence values. We found that 1.1×10^2 parasites were sufficient to

[1] *Abbreviations used:* HFF, human foreskin fibroblast; PDTC, pyrrolidinedithiocarbamate; BKI, bumped kinase inhibitor.

detect the firefly luciferase activity in the bradyzoites (Fig. 1C). Renilla luciferase activity was detected with a minimum of 1.0×10^2 tachyzoites and 1.1×10^2 bradyzoites (Fig. 1C).

Next, we tested PLK/DLUC_1C9 in the microplate format assay. We tested 80 μM ammonium pyrrolidinedithiocarbamate (PDTC, Sigma–Aldrich) as a known bradyzoite-inducing agent [5]. The microplate assay was performed as described in Supplemental Fig. 2. The 80-μM PDTC treatment increased the BAG1 promoter activity by 18-fold when compared with the tachyzoite control (Fig. 2A). We also tested bumped kinase inhibitors (BKIs), which have few sensitive protein kinases in mammalian genome [15] and for which *in vivo* effects have been reported in a mouse infection model [16–18]. TgMAPK1 is a secondary target of BKIs [19], and its involvement in bradyzoite differentiation [20] and cell division [19] has been reported. Three commercial BKIs induced BAG1 promoter activity by approximately 8- to 11-fold (Fig. 2A) when compared with the normal tachyzoite culture conditions (7.8-fold, 1NM-PP1 [Merck]; 8.2-fold, 3MB-PP1 [Toronto Research Chemicals, TRC]); 11-fold, 3BrB-PP1 [TRC]). Accompanying the up-regulation of BAG1 promoter activity, 1NM-PP1-treated parasites formed cyst walls and appeared abnormally large in the parasitophorous vacuoles (Fig. 2B). This large parasite was also reported as an effect to *Neospora caninum* when the parasite was treated with bumped kinase inhibitor 1294 [21]. Therefore, PLK/DLUC_1C9 could detect the BAG1 promoter activation from the induction of cyst genesis by 1NM-PP1.

In summary, our data show that PLK/DLUC_1C9 provides an alternative method for evaluating bradyzoite induction levels in a microplate assay format with normalization via TUBA1 promoter activity and will be of value in revealing the factors affecting bradyzoite differentiation.

Acknowledgments

PLK/hxgprt$^-$ was obtained through the AIDS Reagent Program, Division of AIDS, National Institute of Allergies and Infectious Diseases (NIAID), National Institutes of Health (NIH), from David Roos. SalmonE monoclonal antibody was a kind gift from Louis M. Weiss. We thank T. Tomita for technical advice regarding cyst wall staining. T.S. and F.M. were supported by a Japan Society for the Promotion of Science (JSPS) Research Fellowship for Young Scientists. K.K. was supported by Grants-in-Aid for Young Scientists, Exploratory Research, Scientific Research on Innovative Areas (3308) from the Ministry of Education, Culture, Science, Sports, and Technology (MEXT) of Japan, the Program for the Promotion of Basic and Applied Research for Innovations in Bio-oriented Industry (BRAIN), the Science and Technology Research Promotion Program for Agriculture, Forestry, Fisheries, and Food Industry, and the Program to Disseminate Tenure Tracking System from the Japan Science and Technology Agency (JST). T.M. was supported by JSPS KAKENHI grants (24780295 and 26850183).

Appendix A. Supplementary data

Supplementary data associated with this article can be found, in the online version, at http://dx.doi.org/10.1016/j.ab.2014.06.018.

References

[1] G. Pappas, N. Roussos, M.E. Falagas, Toxoplasmosis snapshots: global status of *Toxoplasma gondii* seroprevalence and implications for pregnancy and congenital toxoplasmosis, Int. J. Parasitol. 39 (2009) 1385–1394.
[2] Y. Carlier, C. Truyens, P. Deloron, F. Peyron, Congenital parasitic infections: a review, Acta Trop. 121 (2012) 55–70.
[3] M.W. Wulf, R. van Crevel, R. Portier, C.G. ter Meulen, W.J. Melchers, A. van der Ven, J.M. Galama, Toxoplasmosis after renal transplantation: implications of a missed diagnosis, J. Clin. Microbiol. 43 (2005) 3544–3547.
[4] M.W. Black, J.C. Boothroyd, Lytic cycle of *Toxoplasma gondii*, Microbiol. Mol. Biol. Rev. 64 (2000) 607–623.
[5] M.S. Behnke, J.B. Radke, A.T. Smith, W.J. Sullivan, M.W. White, The transcription of bradyzoite genes in *Toxoplasma gondii* is controlled by autonomous promoter elements, Mol. Microbiol. 68 (2008) 1502–1518.
[6] K.R. Buchholz, H.M. Fritz, X. Chen, B. Durbin-Johnson, D.M. Rocke, D.J. Ferguson, P.A. Conrad, J.C. Boothroyd, Identification of tissue cyst wall components by transcriptome analysis of in vivo and in vitro *Toxoplasma gondii* bradyzoites, Eukaryot. Cell 10 (2011) 1637–1647.
[7] M.F. Ferreira da Silva, H. Barbosa, U. Gross, C. Lüder, Stress-related and spontaneous stage differentiation of *Toxoplasma gondii*, Mol. Biosyst. 4 (2008) 824–834.
[8] J. Narasimhan, B.R. Joyce, A. Naguleswaran, A.T. Smith, M.R. Livingston, S.E. Dixon, I. Coppens, R.C. Wek, W.J. Sullivan, Translation regulation by eukaryotic initiation factor-2 kinases in the development of latent cysts in *Toxoplasma gondii*, J. Biol. Chem. 283 (2008) 16591–16601.
[9] A. Unno, K. Suzuki, T. Batanova, S. Cha, H. Jang, K. Kitoh, Y. Takashima, Visualization of *Toxoplasma gondii* stage conversion by expression of stage-specific dual fluorescent proteins, Parasitology 136 (2009) 579–588.
[10] H. Zhang, Y. Zhang, J. Cao, Y. Zhou, N. Wang, J. Zhou, Determination of stage interconversion *in vitro* and *in vivo* by construction of transgenic *Toxoplasma gondii* that stably express stage-specific fluorescent proteins, Exp. Parasitol. 134 (2013) 275–280.
[11] M. Di Cristina, D. Marocco, R. Galizi, C. Proietti, R. Spaccapelo, A. Crisanti, Temporal and spatial distribution of *Toxoplasma gondii* differentiation into bradyzoites and tissue cyst formation *in vivo*, Infect. Immun. 76 (2008) 3491–3501.
[12] D.S. Roos, R.G. Donald, N.S. Morrissette, A.L. Moulton, Molecular tools for genetic dissection of the protozoan parasite *Toxoplasma gondii*, Methods Cell Biol. 45 (1994) 27–63.
[13] T. Sugi, K. Kato, K. Kobayashi, S. Watanabe, H. Kurokawa, H. Gong, K. Pandey, H. Takemae, H. Akashi, Use of the kinase inhibitor analog 1NM-PP1 reveals a role for *Toxoplasma gondii* CDPK1 in the invasion step, Eukaryot. Cell 9 (2010) 667–670.
[14] T. Tomita, D.J. Bzik, Y.F. Ma, B.A. Fox, L.M. Markillie, R.C. Taylor, K. Kim, L.M. Weiss, The *Toxoplasma gondii* cyst wall protein CST1 is critical for cyst wall integrity and promotes bradyzoite persistence, PLoS Pathog. 9 (2013) e1003823.
[15] K.K. Ojo, R.T. Eastman, R. Vidadala, Z. Zhang, K.L. Rivas, R. Choi, J.D. Lutz, M.C. Reid, A.M. Fox, M.A. Hulverson, M. Kennedy, N. Isoherranen, L.M. Kim, K.M. Comess, D.J. Kempf, C.L. Verlinde, X.Z. Su, S.H. Kappe, D.J. Maly, E. Fan, W.C. Van Voorhis, A specific inhibitor of *Pf*CDPK4 blocks malaria transmission: chemical–genetic validation, J. Infect. Dis. 209 (2014) 275–284.
[16] T. Sugi, K. Kato, K. Kobayashi, H. Kurokawa, H. Takemae, G. Haiyan, F.C. Recuenco, T. Iwanaga, T. Horimoto, H. Akashi, 1NM-PP1 treatment of mice infected with *Toxoplasma gondii*, J. Vet. Med. Sci. 73 (2011) 1377–1379.
[17] S. Lourido, C. Zhang, M.S. Lopez, K. Tang, J. Barks, Q. Wang, S.A. Wildman, K.M. Shokat, L.D. Sibley, Optimizing small molecule inhibitors of calcium-dependent protein kinase 1 to prevent infection by *Toxoplasma gondii*, J. Med. Chem. 56 (2013) 3068–3077.
[18] J.S. Doggett, K.K. Ojo, E. Fan, D.J. Maly, W.C. Van Voorhis, Bumped kinase inhibitor 1294 treats established *Toxoplasma gondii* infection, Antimicrob. Agents Chemother. 58 (2014) 3547–3549.
[19] T. Sugi, K. Kobayashi, H. Takemae, H. Gong, A. Ishiwa, F. Murakoshi, F.C. Recuenco, T. Iwanaga, T. Horimoto, H. Akashi, K. Kato, Identification of mutations in TgMAPK1 of *Toxoplasma gondii* conferring resistance to 1NM-PP1, Int. J. Parasitol. Drugs Drug Resist. 3 (2013) 93–101.
[20] M.J. Brumlik, S. Wei, K. Finstad, J. Nesbit, L.E. Hyman, M. Lacey, M.E. Burow, T.J. Curiel, Identification of a novel mitogen-activated protein kinase in *Toxoplasma gondii*, Int. J. Parasitol. 34 (2004) 1245–1254.
[21] K.K. Ojo, M.C. Reid, L. Kallur Siddaramaiah, J. Müller, P. Winzer, Z. Zhang, K.R. Keyloun, R.S. Vidadala, E.A. Merritt, W.G. Hol, D.J. Maly, E. Fan, W.C. Van Voorhis, A. Hemphill, Neospora caninum calcium-dependent protein kinase 1 is an effective drug target for neosporosis therapy, PLoS One 9 (2014) e92929.

SCIENTIFIC REPORTS

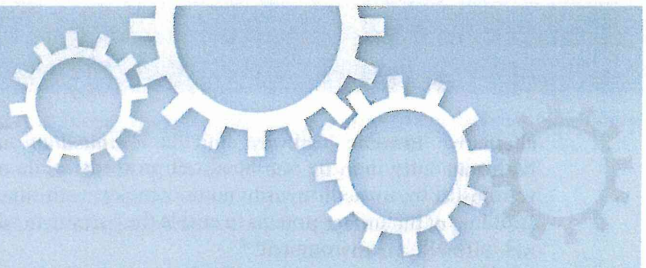

OPEN

SUBJECT AREAS:
PARASITE BIOLOGY
MALARIA
DRUG DEVELOPMENT

Received
27 December 2013

Accepted
1 April 2014

Published
17 April 2014

Correspondence and requests for materials should be addressed to K.K. (kkato@obihiro.ac.jp)

Gellan sulfate inhibits *Plasmodium falciparum* growth and invasion of red blood cells *in vitro*

Frances Cagayat Recuenco[1,2], Kyousuke Kobayashi[3], Akiko Ishiwa[1], Yukiko Enomoto-Rogers[4], Noreen Grace V. Fundador[4], Tatsuki Sugi[1,2], Hitoshi Takemae[1,2], Tatsuya Iwanaga[1], Fumi Murakoshi[1], Haiyan Gong[1], Atsuko Inomata[1], Taisuke Horimoto[1], Tadahisa Iwata[4] & Kentaro Kato[1,2]

[1]Department of Veterinary Microbiology, Graduate School of Agricultural and Life Sciences, The University of Tokyo, 1-1-1 Yayoi, Bunkyo-ku, Tokyo 113-8657, Japan, [2]National Research Center for Protozoan Diseases, Obihiro University of Agriculture and Veterinary Medicine, Inada-cho, Obihiro, Hokkaido 080-8555, Japan, [3]Department of Host-Parasite Interaction, Division of Microbiology and Immunology, Institute of Medical Science, The University of Tokyo, 4-6-1 Shirokanedai, Minato-ku, Tokyo 108-8639, Japan, [4]Laboratory of Science of Polymeric Materials, Department of Biomaterial Sciences, Graduate School of Agricultural and Life Sciences, The University of Tokyo, 1-1-1 Yayoi, Bunkyo-ku, Tokyo 113-8657, Japan.

Here, we assessed the sulfated derivative of the microbial polysaccharide gellan gum and derivatives of λ and κ-carrageenans for their ability to inhibit *Plasmodium falciparum* 3D7 and Dd2 growth and invasion of red blood cells *in vitro*. Growth inhibition was assessed by means of flow cytometry after a 96-h exposure to the inhibitors and invasion inhibition was assessed by counting ring parasites after a 20-h exposure to them. Gellan sulfate strongly inhibited invasion and modestly inhibited growth for both *P. falciparum* 3D7 and Dd2; both inhibitory effects exceeded those achieved with native gellan gum. The hydrolyzed λ-carrageenan and oversulfated κ-carrageenan were less inhibitory than their native forms. *In vitro* cytotoxicity and anticoagulation assays performed to determine the suitability of the modified polysaccharides for *in vivo* studies showed that our synthesized gellan sulfate had low cytotoxicity and anticoagulant activity.

The estimated 660,000 deaths from 220 million cases of malaria reported by the WHO in 2010[1] represents a decline in the mortality caused by malaria especially in the sub-Saharan endemic areas where most cases occur[2]. This success can be attributed to programs that include distribution of insecticide-treated nets, use of indoor residual spraying, and expansion of malarial rapid diagnostic tests. Nevertheless, because of the constant threat of the *Plasmodium* parasites and the *Anopheles* vectors developing resistance to established antimalarials and insecticides, the drive to develop alternative antimalarial drugs, insecticides, and improved rapid diagnostic tests continues[2].

Plasmodium parasites, the causative agent of malaria, are obligate intracellular protozoa transmitted from the blood meal of the female *Anopheles* mosquito to humans. In the erythrocytic stage of the disease, the *Plasmodium* merozoites invade red blood cells, which results in their destruction and the release of the parasite and erythrocytic material into the circulation. The host response to these events manifests into the clinical symptoms of the disease, which include intermittent fever, abdominal pain, anemia, and general weakness[3].

Successful invasion of the erythrocyte is crucial for the survival of the malaria parasite. Upon egress, there is a small window of time when the free malaria merozoites are exposed to the host's immune system, which provides an opportunity to target the parasites with vaccines or drugs[4].

Erythrocyte invasion by the *Plasmodium* merozoite is a complex, multi-step process that involves interactions between the parasite and host cell proteins. The initial reversible attachment of the merozoite to the red blood cell may involve proteins on the merozoite surface, although evidence to support this concept is lacking. During red cell binding, the merozoite reorients so that the apical complex makes contact with the erythrocyte surface. Here, the micronemes secrete invasion proteins, such as apical membrane antigen 1 (AMA1) and erythrocyte binding-like proteins (EBLs), and the rhoptries secrete reticulocyte binding-like proteins (RBLs) and rhoptry neck proteins (RONs). AMA1, a major candidate for a multicomponent vaccine against malaria[5], interacts with the rhoptry neck proteins RON2, RON4, and RON5 to form a complex that is a critical component of the moving junction. The EBLs and RBLs bind with receptors on the red blood cell and are implicated in host cell selection and

alternative invasion pathways for the *Plasmodium* merozoite. Merozoite entry into the red blood cell proceeds as the merozoite is propelled by an actin-myosin motor complex, with simultaneous shedding of the surface proteins to enable the parasite to adapt to its new intracellular environment[6–8].

Sulfated glycosaminoglycans (GAGs), such as heparin[9], dextran sulfate, fucoidan[10,11], and fucosylated chondroitin sulfate[12] have been shown to inhibit merozoite entry into erythrocytes *in vitro*. In addition, sulfated GAGs have been shown to prevent the cytoadherence of *Plasmodium*-infected red blood cells *in vitro*[10–15].

Heparin, in particular, appears to target several merozoite proteins[16,17], including invasion proteins such as merozoite surface protein 1 (MSP1)[18] and erythrocyte binding antigen 140 (EBA-140)[19]. Thus, unlike other antimalarials, heparin can inhibit the invasion of red blood cells by the *Plasmodium* merozoites[20]. MSP1 is a major candidate for a multi-component malaria vaccine[5], and EBA-140, also known as BAEBL, is an erythrocyte binding ligand that interacts with the glycophorin C receptor on the erythrocyte surface[21]. These findings provide clues as to how these invasion proteins interact with cell surface proteoglycans, such as heparan sulfate, and could help explain the mechanism by which sulfated polysaccharides inhibit parasite entry into red blood cells. However, because heparin is a potent anticoagulant, it cannot be used to treat clinical malaria[22].

Sulfated polysaccharides from marine sources are currently being exploited for their potential therapeutic applications. These include carrageenans from seaweeds, of which there are three major types: kappa (κ), lambda (λ), and iota (ι). These carrageenans differ in their levels of sulfation, which may also account for their different gelling properties. The carrageenans inhibit *P. falciparum* 3D7 and Dd2 growth and invasion of red blood cells *in vitro*[23]. *In vivo*, A/J mice pre-treated with calcium carrageenan prior to infection with *P. berghei* NK65A showed lower parasitemia compared with the untreated group but this pre-treatment did not promote recovery or survival of the animals[24]. In addition, Huber *et al.*[25] showed that there was an increase in the permeability of the blood brain barrier in rats 72 h after subcutaneous administration of λ-carrageenan. This side effect could enhance the development of cerebral malaria and is thus a major disadvantage of carrageenans for therapeutic use in malaria.

Modification of κ-carrageenan improved its potential for use against various pathogens. The basic structure of κ-Carrageenan consists of (1 → 3)-β-D-galactose (G unit) - (1 → 4)-α- 3,6-anhydro D-galactose (A unit). Acetylated, sulfated, and phosphorylated κ-carrageenan derivatives show enhanced antioxidant and antitumor properties[26]. Other κ-carrageenan derivatives have shown activity against tumor cells[27,28], bacteria[29] and viruses, including influenza virus[30,31], and human immunodeficiency virus[32]. We, therefore, sought to determine whether modification of κ-carrageenan and λ-carrageenan could affect their action against malaria parasites and their safety as potential adjunct therapy for malaria.

Gellan gum (GG) is a linear, anionic, high molecular weight, microbial polysaccharide produced by the bacterium *Sphingomonas* (*Pseudomonas*) *elodea* (ATCC 31461). It is a thermoreversible gel, noted for its high gel strength and stability, which make it useful as a drug vehicle, food additive, component of personal care products, and microbiological media. Its basic repeating unit is a tetrasaccharide, consisting of two glucose (Glc) residues, one glucuronic acid (GlcA), and one rhamnose (Rha) residue: [→3)-β-D-Glc*p*-(1 → 4)-β-D-Glc*p*A-(1 → 4)-β-D-Glc*p*-(1 → 4)-α-L-Rhap-(1→][33–36]. Animals studies involving gellan gum addition to the diet or being given by gavage have shown it to be inert and safe for internal use[35]. *In vivo*, GG has been found to have low induction of inflammation, so GG-based materials have been evaluated for potential therapeutic applications that include films to reduce post-surgical adhesions[37–39] and discs for nucleus pulposus regeneration[40]. GG-based hydrogels were also found to support viability of encapsulated chondrocytes intended for cartilage transplants[41].

Gellan gum has been modified to obtain sulfated derivatives (gellan sulfate)[42] that have anticoagulant activities similar to those of heparin, with the exception of one derivative (GS1), which had the lowest sulfonation ratio (5.0%), and the least anticoagulant activity[43]. The *in vivo* effects of gellan sulfate, however, appear not to have been fully explored yet. To our knowledge, there are no published reports on the *in vitro* effects of gellan gum and gellan sulfate on malaria parasites.

The goal of this study was to assess synthetic compounds that inhibit merozoite entry into red blood cells, similarly to heparin, but with a better safety profile. We evaluated the microbial polysaccharide gellan gum and prepared its sulfated derivative, gellan sulfate, and the carrageenan derivatives, hydrolyzed λ-carrageenan and oversulfated κ-carrageenan, for their inhibitory effects on *Plasmodium falciparum* 3D7 and Dd2 growth and invasion of erythrocytes. We also tested these compounds for their cytotoxicity to 293T cells. In addition, we assessed the *in vitro* anticoagulant activity of our synthesized gellan sulfate for its suitability for *in vivo* studies.

Results

Synthesis of gellan gum, λ- and κ-carrageenan derivatives. κ-Carrageenan and gellan gum were sulfated by the SO_3-pyridine complex. The κ-carrageenan and gellan sulfates, and the hydrolyzed λ-carrageenan were more readily soluble in distilled water at room temperature compared with their native counterparts. The modified polysaccharides also did not form gels in solution.

The degree of substitution (DS) of the sulfonyl group and sulfation rate (%) were determined by elemental analyses and are listed in Table 1. The DSs for κ-carrageenan and gellan were defined as the molar number of sulfonyl group per di-saccharide and tetra-saccharide unit, respectively.

NMR analyses were used to confirm the sulfation of κ-carrageenan and gellan. ^{13}C-NMR spectra before and after sulfation are available in the Supplemental data (Supplementary Figs. S1 and S2). The peaks of native κ-carrageenan and gellan were assigned according to the assignments reported previously[44–46]. The major peaks of sulfated κ-carrageenan with a DS of 3.0 were also assigned according to the assignments for sulfated κ-carrageenan with a DS of 3.1 reported elsewhere[47,48]. The overlapped peaks of ring-carbons of gellan sulfate with a DS of 3.7 were rarely assigned due to their complex appearance caused by sulfonyl substituents and remaining hydroxyl groups. In the case of κ-carrageenan, shifts of the peaks of C6 (G) from 61.4 to 66.5 ppm, C2 (G) from 69.7 to 75.4 ppm and C2 (A) from 70.0 to 72.7 ppm indicated successful sulfation at these positions. The complete disappearance of the peak assigned C6 (G) indicated that the C6 (G) position was completely substituted. Other peaks were likely assigned to ring carbons of un-substituted sugar units. In the case of gellan, the peaks assigned to C6 (13 G) at 61.7 ppm, C6 (14 G) at 62.2 ppm, C2 (R) at 71.6 ppm, and C3 (R) at 71.7 ppm, completely disappeared, indicating preferential sulfation at these positions.

Table 1 | Characteristics of sulfated κ-carrageenan and gellan gum

Sulfated derivatives	Elemental analysis (%) C	H	S	DS[a]	Sulfation rate (%)[a]
κ-carrageenan	20.3	4.09	13.6	3.0	75
Gellan	23.3	4.38	9.57	3.7	37

[a]Relative to maximun DS: 4.0 (κ-carrageenan), 10.0 (gellan).
DS – degree of substitution.
Percent carbon (C), hydrogen (H), and sulfur (S) as determined by elemental analyses. DS was calculated according to the equation of Rochas, *et al.*[45], that is, DS = (S%/atomic mass of S)/(C%/atomic mass of C × number of carbons for one unit). Sulfation rate (%) was calculated by taking the ratio of the DS of the sulfonyl group to the maximum DS of 4.0 for κ-carrageenan and 10.0 for gellan.

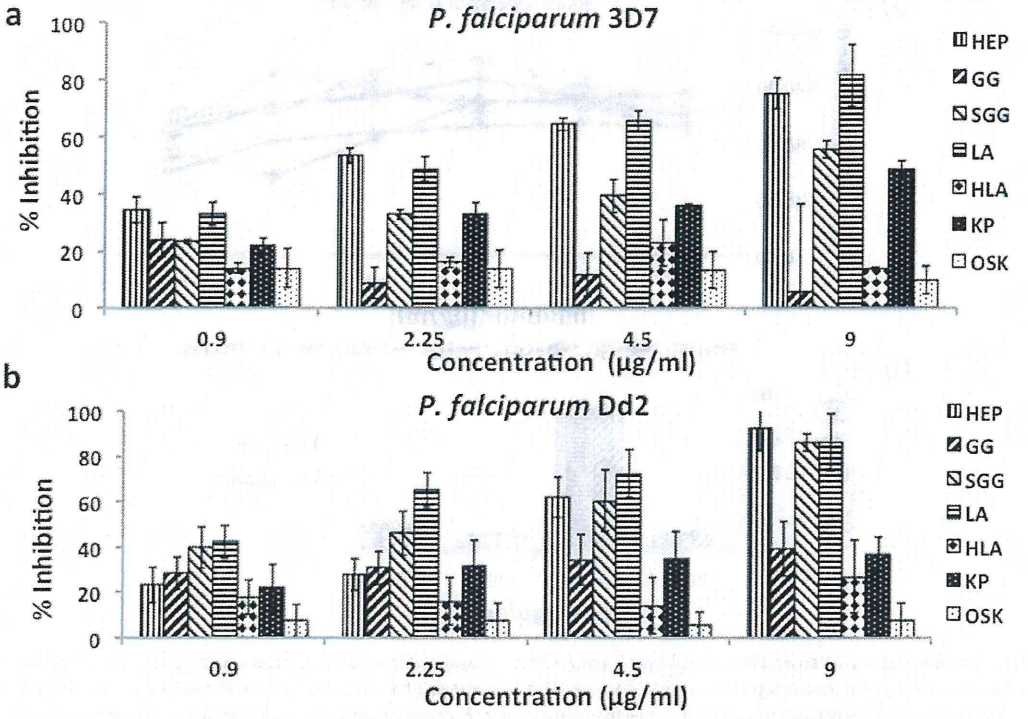

Figure 1 | *In vitro* growth inhibition of *P. falciparum* 3D7 (A) and Dd2 (B). Late stage *P. falciparum* 3D7 and Dd2 trophozoites (parasitemia 0.3%, hematocrit 1%) were cultured in the presence of the following inhibitors: heparin (HEP), gellan gum (GG), gellan sulfate (SGG), λ-carrageenan (LA), hydrolyzed λ-carrageenan (HLA), κ-carrageenan (KP), and oversulfated κ-carrageenan (OSK) in 96-well round-bottom plates for 96 h. Final parasitemia was determined by use of flow cytometry. Percent inhibition is shown (y-axis) against increasing concentrations (x-axis) of each inhibitor. At 9 µg/ml, SGG inhibited the growth of *P. falciparum* 3D7 by 55.33% and that of Dd2 by 85.83%. At the same concentration, GG, HLA, and OSK inhibited both *P. falciparum* lines by 20% or less. Error bars represent standard deviations from the means of triplicate assays from three independent experiments.

Growth inhibition assay. The native λ- and κ−carrageenans inhibited the growth of *P. falciparum* 3D7 (Figure 1A) and Dd2 (Figure 1B) *in vitro* in a concentration-dependent manner consistent with the observations of Adams *et al.*[23]. Both the hydrolyzed λ-carrageenan and the oversulfated κ-carrageenan derivatives poorly inhibited *P. falciparum* 3D7 and Dd2 growth *in vitro*. Gellan sulfate (9 µg/ml) inhibited growth of *P. falciparum* 3D7 (55.33%) and Dd2 (85.83%) *in vitro* (Figure 1A and 1B). In contrast, native gellan gum exhibited low inhibition (5.58%, 3D7; and, 39.22%, Dd2) at the same concentration. We, therefore, chose to assess gellan sulfate and the native gellan gum for their ability to inhibit invasion.

Invasion inhibition assay. At 10 µg/ml, gellan sulfate showed strong inhibition of invasion by *P. falciparum* 3D7 (93.92%) and Dd2 (88.39%) *in vitro* (Figure 2). Heparin also showed inhibition of invasion by *P. falciparum* 3D7 (69%) and Dd2 (89.03%). Native gellan gum showed moderate inhibition of invasion for both *P. falciparum* 3D7 and Dd2 (46.13% and 47.51%).

Cytotoxicity assays. Unlike native gellan gum, gellan sulfate does not gel in solution. With this change in property, we wanted to determine the safety of gellan sulfate for future *in vivo* studies. Hence, we performed MTT cytotoxicity assays on 293T cells using the original selection of inhibitors for comparison (Figure 3A). Heparin and native gellan gum treatment caused a marked decrease in cell viability at concentrations of 250 and 500 µg/ml (54.68% and 70.18% for heparin; 79.86% and 57.74% for gellan gum). By contrast, gellan sulfate, as well as the native λ- and κ- carrageenans and their respective derivatives, showed relatively low cytotoxicity at 500 µg/ml (86.44%, 81.52%, 89.33%, 101.88%, and 94.30%, respectively).

***In vitro* anticoagulant activity of gellan sulfate.** The *in vitro* anticoagulant activity of the gellan sulfate was assessed by using activated partial thromboplastin time (APTT) anticoagulant assays with healthy mouse plasma[49]. In separate experiments, the APTT values for normal plasma from a healthy animal ranged from 16.0 s to 27.1 s, with a mean value of 23.4 s. The APTT for plasma with heparin at 10 and 100 µg/ml increased dramatically (mean = 181.0 s), whereas mean APTTs for plasma with 10 and 100 µg/ml

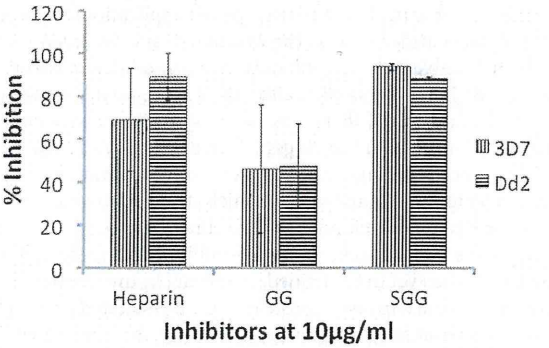

Figure 2 | *In vitro* invasion inhibition of *P. falciparum* 3D7 and Dd2. MACS-purified *P. falciparum* 3D7 and Dd2 schizonts were cultured in 96-well plates (ring stage parasitemia = 0%, hematocrit = 1%) for 20 h in the presence of 10 µg/ml heparin, gellan gum (GG), and gellan sulfate (SGG). Ring stage parasitemia were counted using Giemsa stained smears. Percent inhibition of invasion of *P. falciparum* 3D7 and Dd2 are shown. Error bars represent standard deviations from the means of duplicate assays from two independent experiments.